The Plant Cell, Vol. 14, 2045–2058, September 2002, www.plantcell.org © 2002 American Society of Plant Biologists

The Identification of *CVP1* Reveals a Role for Sterols in Vascular Patterning

Francine M. Carland,[a] Shozo Fujioka,[b] Suguru Takatsuto,[c] Shigeo Yoshida,[b] and Timothy Nelson[a,1]

[a] Department of Molecular, Cellular, and Developmental Biology, Yale University, New Haven, Connecticut 06511
[b] Institute of Physical and Chemical Research, Wako-shi, Saitama 351-0198, Japan
[c] Department of Chemistry, Joetsu University of Education, Joetsu-shi, Niigata 943-8512, Japan

Vascular cell axialization refers to the uniform alignment of vascular strands. In the Arabidopsis *cotyledon vascular pattern1* (*cvp1*) mutant, vascular cells are not arranged in parallel files and are misshapen, suggesting that *CVP1* has a role in promoting vascular cell polarity and alignment. Characterization of an allelic series of *cvp1* mutations revealed additional functions of *CVP1* in organ expansion and elongation. We identified *CVP1* and found that it encodes STEROL METHYLTRANSFERASE2 (SMT2), an enzyme in the sterol biosynthetic pathway. SMT2 and the functionally redundant SMT3 act at a branch point in the pathway that mediates sterol and brassinosteroid levels. The *SMT2* gene is expressed in a number of developing organs and is regulated by various hormones. As predicted from SMT2 enzymatic activity, the precursors to brassinosteroid are increased at the expense of sterols in *cvp1* mutants, identifying a role for sterols in vascular cell polarization and axialization.

INTRODUCTION

The plant vascular system is formed progressively during embryogenesis and postembryonic development. In organ primordia, provascular cells appear among ground cells in hierarchical patterns that give rise to the patterns of veins (Nelson and Dengler, 1997). Provascular cells proliferate and elongate in axialized files that appear to depend on the intercellular polar transport of auxin through the developing tissue. Screens for pattern-defective mutants have identified several genes that regulate or influence this process. The *monopteros* mutation causes a discontinuous venation pattern associated with improper vascular differentiation (Przemeck et al., 1996) and corresponds to an auxin response transcription factor (Hardtke and Berleth, 1998).

In *gnom/emb30* mutants, which correspond to a brefeldin A–sensitive ADP-ribosylation factor guanine-nucleotide exchange factor (ARF-GEF), veins are unaxialized and patterned irregularly (Mayer et al., 1993; Shevell et al., 1994; Steinmann et al., 1999; Grebe et al., 2000; Koizumi et al., 2000). Additional venation pattern mutants have been described, such as the *van* mutants, *lop1*/*tornado1*, and *scarface*, but their gene products have not been identified (Carland and McHale, 1996; Cnops et al., 2000; Deyholos et al., 2000; Koizumi et al., 2000).

[1] To whom correspondence should be addressed. E-mail timothy.nelson@yale.edu; fax 203-432-5632.
Article, publication date, and citation information can be found at www.plantcell.org/cgi/doi/10.1105/tpc.003939.

We recently described a number of additional mutants with various effects on cotyledon vascular pattern (Carland et al., 1999). One of these, *cotyledon vascular pattern1* (*cvp1*), resembles the *monopteros* phenotype in that a discontinuous, poorly axialized venation pattern is formed. Here, we show that *cvp1* corresponds to a defect in sterol biosynthesis.

Derivatives of the sterol pathway in plants and animals include both membrane sterols and signaling steroids. Recently, the membrane sterol cholesterol was shown to influence signaling and vectorial processes through its key role in the organization of lipid rafts (Simons and Ikonen, 1997). Lipid rafts appear to provide scaffolding for protein localization and distribution, membrane trafficking, and membrane signaling (Simons and Toomre, 2000). Although such rafts have not yet been described in plants, the diversity of plant sterols makes the possibility intriguing, particularly in highly polarized cells such as those in procambial strands.

In contrast to animals and fungi, in which a single major sterol is accumulated, plants accumulate many sterols (Hartmann, 1998). The most abundant plant sterols differ mainly by the number of carbon additions at the C-24 position, which are catalyzed by sterol methyltransferases (SMTs) in an *S*-adenosyl Met–dependent manner (Benveniste, 1986). In Arabidopsis, there are three SMTs, each of which can complement the defects in yeast SMT-deficient *erg6* mutants (Husselstein et al., 1996; Bouvier-Nave et al., 1997; Diener et al., 2000). SMT1, which is the most homologous with yeast ERG6, catalyzes the initial sterol methyltransfer reaction and serves as a branch point between cholesterol

and the more abundant sterols and brassinosteroids (BRs) (Diener et al., 2000). SMT2 and SMT3 catalyze a second methyltransfer, which distinguishes the sterols from BR precursors (Bouvier-Nave et al., 1997). As a result of SMT activities, cholesterol, stigmasterol, campesterol, and sitosterol accumulate (in order of increasing abundance), as do a number of downstream derivatives.

The phenotypes of sterol biosynthetic mutants suggest that there are diverse sterol-dependent processes. The single SMT1 in yeast is defined by *erg6* mutants, which were recovered in mutant screens for impaired Trp uptake, increased resistance to polyene antibiotics, hypersensitivity to various metals and ion salts, sensitivity to brefeldin A, suppression of vesicle trafficking, decreased mating efficiency, and modulation of steroid receptor signaling (Parks et al., 1999). The causality between sterol deficiency and phenotype may have a different basis in each case and is unlikely to be limited to alterations in membrane rigidity or permeability. Arabidopsis *smt1* mutants, in which cholesterol is aberrantly abundant, have compact rosettes, slightly reduced plant statures with blunt siliques, and a conditional root growth defect (Diener et al., 2000). Tobacco plants that overexpress soybean SMT1 have decreased cholesterol and increased sitosterol and 24-methyl cholesterol without significant effects on plant growth and development (Sitbon and Jonsson, 2001).

Antisense SMT2 plants, which have lower sterol levels and higher campesterol levels, exhibit dwarfism accompanied by reduced apical dominance, floral organ elongation, and fertility (Schaeffer et al., 2001). Plants that overexpress SMT2 contain higher levels of sitosterol and lower levels of campesterol and exhibit reduced plant stature that can be rescued with exogenous application of BRs (Schaeffer et al., 2001). *fackel* mutants, which are defective in C-14 reductase, display altered embryonic and postembryonic patterning, including a vascular patterning defect, as a result of abnormal cell division and expansion. In *fackel* mutants, both BRs and sterols after the defective step are reduced and uncommon 8,14-diene sterols accumulate (Jang et al., 2000; Schrick et al., 2000).

We cloned the gene that corresponds to the *cvp1* mutant described above and found that it encodes the Arabidopsis C-24 SMT2. As predicted from the role of SMT2 in the sterol biosynthetic pathway, sterol levels were altered significantly. Based on the phenotypes of an allelic series of *cvp1* mutants, we propose that *cvp1* mutants are defective in sterol signaling or an aspect of membrane organization that is essential for the polarization and axialization of vascular cells.

RESULTS

Additional Alleles of *cvp1* Exhibit Defects Consistent with Aberrant Cell Expansion and Cell Elongation

As reported previously, four alleles of *cvp1* (*cvp1-1*, *cvp1-2*, *cvp1-3*, and *cvp1-4*) were identified from a screen of >34,000 ethyl methanesulfonate–mutagenized M2 seedlings derived from 10 M1 pools (Carland et al., 1999). *cvp1-1* and *cvp1-2* showed identical phenotypes and were found to have the same mutation (described below). Therefore, we compared in detail only the phenotypes of *cvp1-1*, *cvp1-4*, and *cvp1-3*, which correspond to weak, intermediate, and strong alleles, respectively.

All *cvp1* alleles exhibited a discontinuous cotyledon venation pattern that consisted of isolated patches (Figures 1A to 1D) of vascular tissue that lacked cellular axialization. There was a reduction of vein loops in cotyledons of *cvp1-4* and *cvp1-3*, and the veins were thicker. The reduced cotyledon expansion of *cvp1-4* and *cvp1-3* in the proximal-distal axis resulted in a "soup spoon"–shaped cotyledon. *cvp1-3* cotyledons were smaller than those of the wild type. No vascular aberrations were apparent in the rosette leaves of the *cvp1* alleles (Figures 1E to 1H). Flowers in all *cvp1* alleles were normal in gross morphology. However, petals appeared scalloped, with highly serrated margins (Figures 1I and 1J), and sepals were highly serrated, with ectopic protrusions extending from the apical margins (Figures 1K and 1L). These affected foliar organs often exhibited vascular alterations such as vein regions with nonuniform thickening.

cvp1-1 and *cvp1-4* were similar to wild-type plants in general morphology and growth rate (Figure 1N), whereas *cvp1-3* plants had retarded growth and were smaller at both the seedling and rosette stages (Figures 1M and 1N). The compact *cvp1-3* rosette was composed of small vegetative leaves that failed to expand to wild-type size. This strong *cvp1-3* allele also exhibited delayed flowering time and senescence and reduced plant height and apical dominance.

cvp1 siliques were shorter (wild type, 13.1 $\pm$ 1.1 mm; *cvp1*, 10.1 $\pm$ 0.5 mm [$n = 61$ siliques from 12 plants]) and wider than wild-type siliques (Figure 1O). However, a reduction in fertility occurred only in the strong *cvp1-3* allele. As described previously, *cvp1-1* had a decrease in internodal stem elongation in the apex of primary and secondary inflorescences in $\sim$10% of the inflorescence stems. Transverse sections of stem tissue within this mutant region revealed an overproliferation of lignified tissue (Carland et al., 1999). This phenotype occurred at a higher frequency in *cvp1-3*, affecting 55% of plants (77 of 139) (Figure 1P). In summary, in addition to the loss of vascular cell axialization, strong *cvp1* mutants exhibited defects in elongation at the cellular level (vascular cells) and/or the organ level (stem and siliques) and an expansion defect similar to that seen in leaves.

CVP1 Encodes SMT2

We previously mapped *CVP1* to chromosome 1 near *MONOPTEROS* between m59 and m235 (Hardtke and Berleth, 1998). To clone *CVP1*, a large mapping population was generated and scored for recombinants, as diagrammed in Figure 2A. Polymorphic markers were designed based on limited sequence data in the region and used to further localize

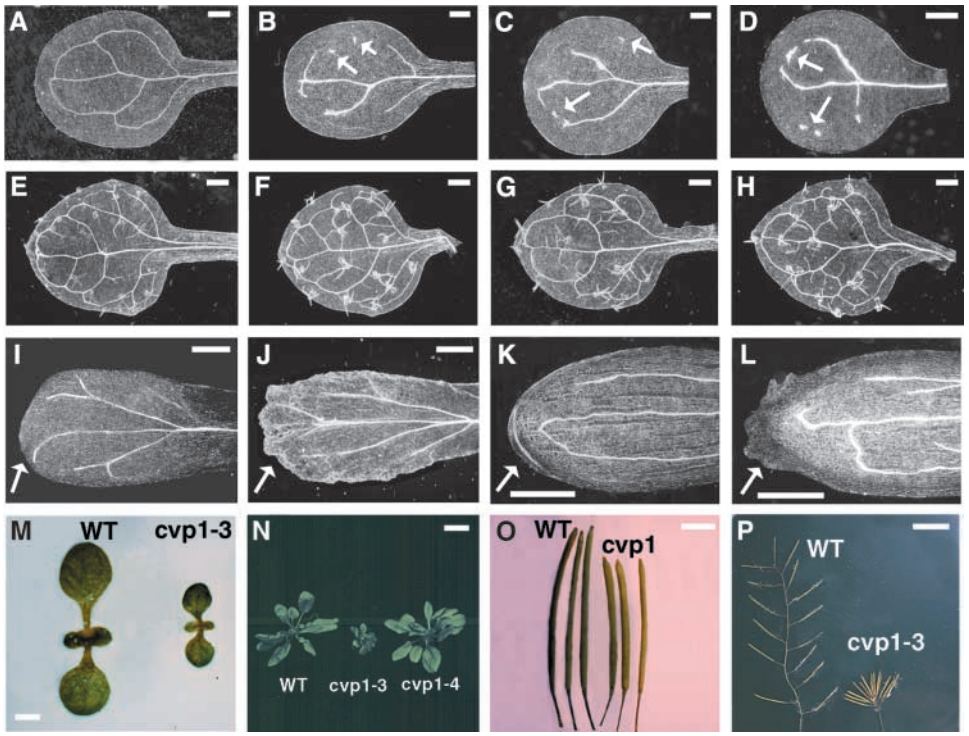

Figure 1. Phenotypes of *cvp1* Alleles.

(A) to **(H)** Venation patterns of cleared cotyledons **(A)** to **(D)** and first rosette leaves **(E)** to **(H)** viewed under dark-field illumination. Arrows denote vascular discontinuities.
(A) and **(E)** Wild type (Columbia ecotype).
(B) and **(F)** *cvp1-1*.
(C) and **(G)** *cvp1-4*.
(D) and **(H)** *cvp1-3*.
(I) to **(L)** Margins of cleared petals **(I)** and **(J)** and sepals **(K)** and **(L)** viewed under dark-field illumination. Arrows indicate smooth margins of the wild type in contrast to the marginal protrusions of *cvp1-1*.
(I) and **(K)** Wild type.
(J) and **(L)** *cvp1-1*.
(M) Seven-day-old seedlings of the wild type (WT) and *cvp1-3*. The growth of *cvp1-3* is retarded, and seedlings are smaller than those of the wild type.
(N) Vegetative stage of wild-type, *cvp1-3*, and *cvp1-4* plants. *cvp1-4* is indistinguishable from the wild type, but *cvp1-3* has a compact rosette.
(O) Siliques of the wild type and *cvp1*. *cvp1* mutant siliques are shorter and wider than wild-type siliques.
(P) Inflorescence stem internodal elongation defect in *cvp1-3* compared with that of the wild type. Nodes between siliques fail to elongate, resulting in a cluster of siliques.
Bars in **(A)** to **(D)** and **(I)** to **(L)** = 250 μm; bars in **(E)** to **(H)** = 500 μm; bar in **(M)** = 1 mm; bar in **(N)** = 1.5 cm; bar in **(O)** = 3 mm; bar in **(P)** = 1 cm.

CVP1 to two overlapping BACs. PCR products were amplified from the unordered BAC sequences and used as probes to screen a transformation-competent artificial chromosome (TAC) library (Liu et al., 1999), resulting in an ordered contig of TAC clones spanning the *CVP1* region.

Individual TAC clones were introduced into *cvp1-1* mutants and scored for complementation of the *cvp1* mutant phenotype. A complementing TAC contained six unique genes relative to overlapping noncomplementing TACs, based on gene annotation that had become available by that date. These six genes were sequenced in the *cvp1-1* background, and a mutation was identified in a previously identified gene encoding SMT2 (Bouvier-Nave et al., 1997). The additional *cvp1* alleles contained mutations in this gene. *cvp1* was complemented by transformation with the *SMT2* genomic region, confirming the identity of *CVP1* (Figure 2B).

Although *cvp1-1* and *cvp1-2* were identified from different M1 pools and therefore should be independent alleles, they contain the same mutation in an invariant residue within the first *S*-adenosyl Met binding site. *cvp1-4* was found to have a nonsense mutation that is predicted to produce a truncated protein. The *cvp1-3* allele contained a missense

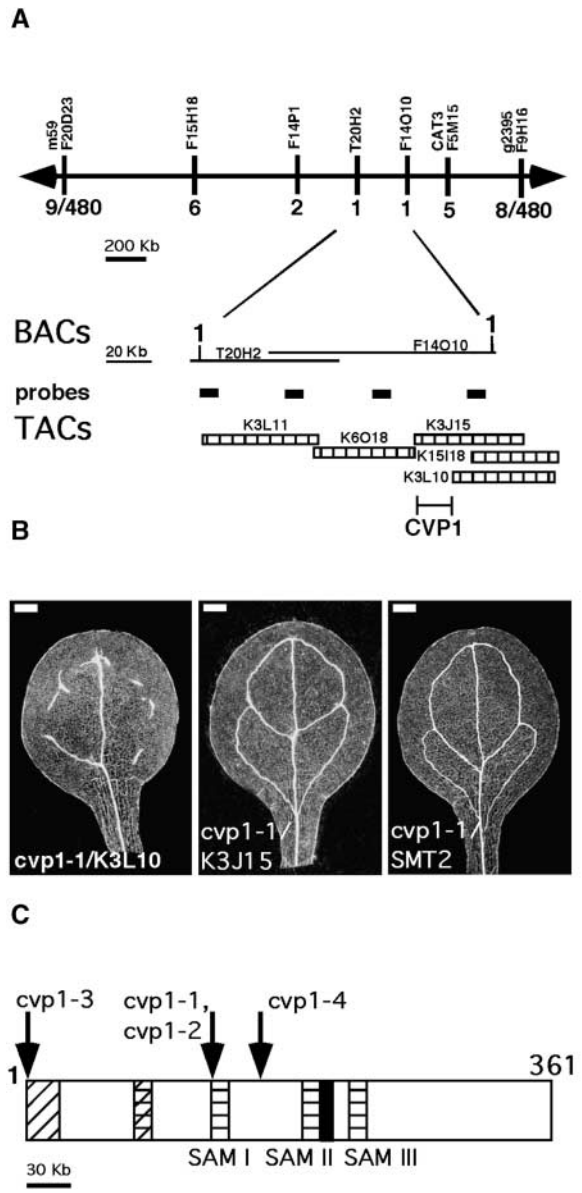

Figure 2. Positional Cloning of *CVP1*.

(A) Line drawing of *CVP1* cloning strategy. *cvp1* in the Columbia background was crossed to the polymorphic ecotype Landsberg *erecta* to generate a mapping population of 480 meiotic events. Using breakpoint analysis, *CVP1* was positioned on chromosome 1 between cleaved amplified polymorphic markers m59 and g2395. The numbers of recombinants between *CVP1* and polymorphic flanking markers are shown below the line with double arrows. The BACs from which markers were designed are noted at top. *CVP1* was localized to the two overlapping BACs, T20H2 and F14O10. Probes designated by small thick lines were generated from these BACs and used to identify overlapping TAC clones as labeled. Only the TAC clones that yielded transgenic plants are shown.

(B) Complementation of *cvp1*. One TAC clone complemented the *cvp1-1* mutant vascular patterning defect (K3J15) and contained six unique annotated genes relative to a noncomplementing TAC clone (K3L10). A genomic clone of *SMT2* was generated and shown to complement *cvp1*. Bars = 250 μm.

(C) Gene structure with mutations. Motifs proposed to be functionally important, as listed from amino acid 1, are as follows: the hatched box represents the signal anchor; the box with diagonal and horizontal lines indicates the sterol binding site (Nes et al., 1999); the black box denotes a conserved region among SMTs of unknown function; *S*-adenosyl Met (SAM) sites are labeled boxes. Mutations within the *cvp1* alleles are denoted. Specifically, *cvp1-3* has a G-to-A nucleotide substitution in the initiation codon, changing Met to Ile. *cvp1-1* and *cvp1-2* are independent alleles that have a G-to-A nucleotide substitution, changing Asn to Asp. *cvp1-4* has a C-to-T nucleotide substitution, resulting in an early termination codon.

mutation in the initiation codon (Figure 2C) that should result in a null allele, consistent with its more severe phenotype. The next in-frame Met residue follows the sterol binding site.

Features of the SMT2 Protein

SMT2 is one of three SMT enzymes in Arabidopsis, all of which share regions of homology. SMT1 has substrate affinities that differ from those of SMT2 and SMT3 and acts earlier in the sterol biosynthetic pathway (Figure 3). SMT2 and SMT3 are 83% identical in amino acid sequence and act on the same substrate at the pathway bifurcation that distinguishes sterols from BRs. The predicted protein structure of SMT2 includes a hydrophobic region at the N terminus (Figure 2C). This region meets the criteria for a signal anchor (as predicted with SignalP [http://www.cbs.dtu.dk/services/SignalP]) and may serve to direct SMT2 to the endoplasmic reticulum, where sterol biosynthesis is postulated to occur. The sequence predicts three sites for binding of *S*-adenosyl Met, the methyl donor for SMT reactions, a sterol binding site (Nes et al., 1999), and a region of unknown function conserved among all SMTs.

SMT2 Is Expressed in Several Developing Organs

We examined the effects of the *cvp1* molecular lesions on *SMT2* transcript levels by RNA gel blot analysis. RNA isolated from 6-day-old seedlings revealed decreases in *SMT2* transcript levels in all alleles (Figure 4A) in proportion to their phenotypic severity, even though the mutations were predicted to alter translational products rather than transcription. There were undetectable levels of *SMT2* transcripts in the severe *cvp1-3* allele, confirming the designation of *cvp1-3* as a null allele.

The *cvp1* mutations in *SMT2* also affected the accumulation of transcripts for *SMT1* and *SMT3*. The transcript levels of the highly homologous SMT3 and of SMT1, determined with gene-specific probes, were increased in *cvp1-4* but

were unaffected in *cvp1-1*. Remarkably, neither transcript was detected in *cvp1-3*, suggesting that the null allele is deficient in all SMT activity. We reproduced these measurements several times, because the results were unexpected. Some effects on *SMT2* and *SMT3* transcript levels were reported previously for *smt1* mutants, but these were not as great as the effects we observed in *cvp1* alleles (Diener et al., 2000). The increased *SMT1* and *SMT3* transcript levels in *cvp1-4* and the decreases in *cvp1-3* may reflect a feedback mechanism between sterol production and activation of the *SMT* genes. Alleles that differ in severity may disrupt domains in SMT2 involved in distinct aspects of this regulation.

The *SMT2* gene was expressed in most developing tissues in a pattern that differed slightly from that of *SMT3* and *SMT1*. RNA gel blot analysis showed that *SMT2* mRNA was present in all developing tissues surveyed and revealed low-level expression in roots and siliques, moderate levels in seedling and rosette leaves, and abundant levels in stems and inflorescences (Figure 4A). *SMT3* showed a similar expression profile, except that mRNA was at undetectable levels in siliques (Figure 4B). Likewise, the pattern of *SMT1* mRNA (data not shown) resembled that of SMT2, in agreement with a previous report (Diener et al., 2000).

The expression of *SMT2* was influenced by several hormones. We measured *SMT2* and *SMT3* mRNA after treatment with ethylene, cytokinin, indoleacetic acid, epibrassinolide, or gibberellic acid, as described in Methods. Hormone induction studies indicated that *SMT2* was induced strongly and moderately by ethylene and cytokinin, respectively. *SMT3* was induced strongly by cytokinin. *SMT2* and *SMT3* were induced weakly and moderately, respectively, by indoleacetic acid. The BR epibrassinolide and gibberellic acid did not appear to have any effect on *SMT* transcript levels. This finding suggests that *SMT2* and *SMT3* are induced differentially by at least three hormones that promote cell division and/or elongation.

SMT2 appeared to be expressed predominantly in regions with active cell division. We visualized *SMT2* mRNA accumulation by in situ RNA hybridization (Figure 5). As reported previously (Diener et al., 2000), *SMT2* was expressed throughout the developing embryo (Figure 5A). In agreement with the RNA gel blot studies, *SMT2* was expressed in a number of nascent organs. These included the primordia of leaves, sepals, stamens, gynoecia (Figures 5B to 5E), and petals (data not shown). *SMT2* also was expressed in the inflorescence meristem (Figure 5C) and in developing ovules (Figure 5F). *SMT2* expression at these sites was limited in each case to stages that included actively dividing cells.

β-Glucuronidase (GUS) reporter analysis revealed some additional features of the *SMT2* and *SMT3* expression patterns. Both were expressed specifically in the elongation zone of the roots (Figures 6A and 6B). In rosettes, GUS histochemical staining was apparent in cotyledons, expanding leaves, and the apical tips of young leaves (Figures 6C and 6D). These are regions in the leaf that are undergoing cell expansion and reflect the basipetal maturation of leaves. In

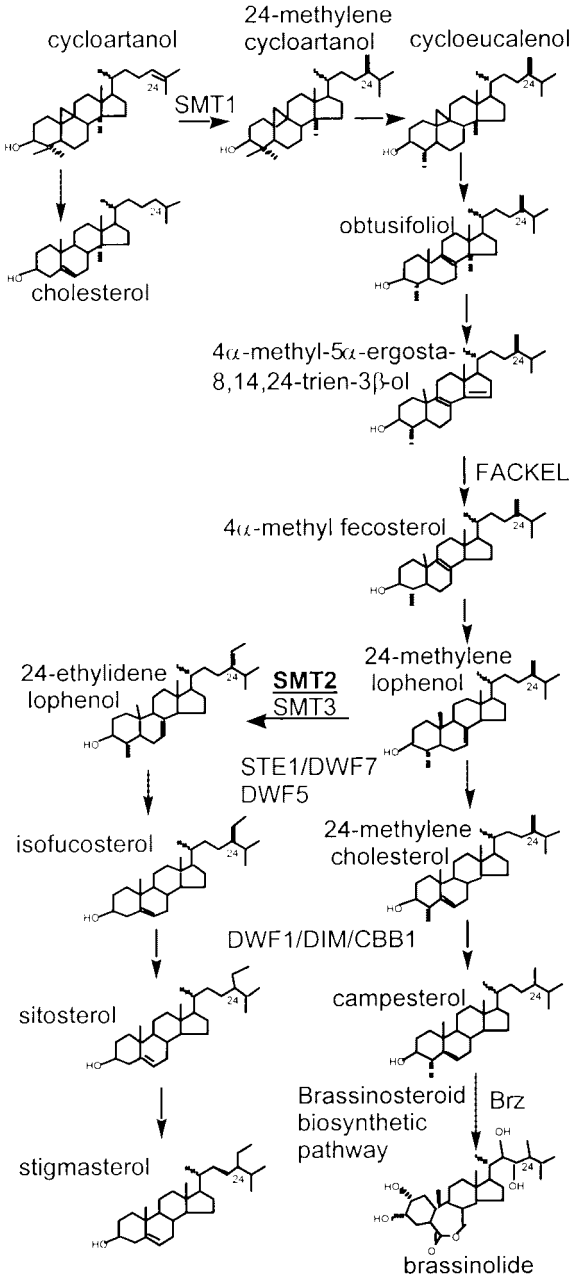

Figure 3. The Sterol Biosynthetic Pathway.

A simplified version of the sterol biosynthetic pathway is shown. Sterol intermediates are labeled. Genes that are enzymes and that have been identified by mutation, with the exception of *SMT3*, are shown in uppercase letters (Klahre et al., 1998; Choe et al., 1999a, 1999b, 2000; Diener et al., 2000; Jang et al., 2000; Schrick et al., 2000). The site of SMT methyl addition, C-24, is indicated. SMT2 is shown in boldface and underlined. Brz is a BR biosynthetic inhibitor (Asami and Yoshida, 1999). Dashed arrows indicate multiple biosynthetic steps.

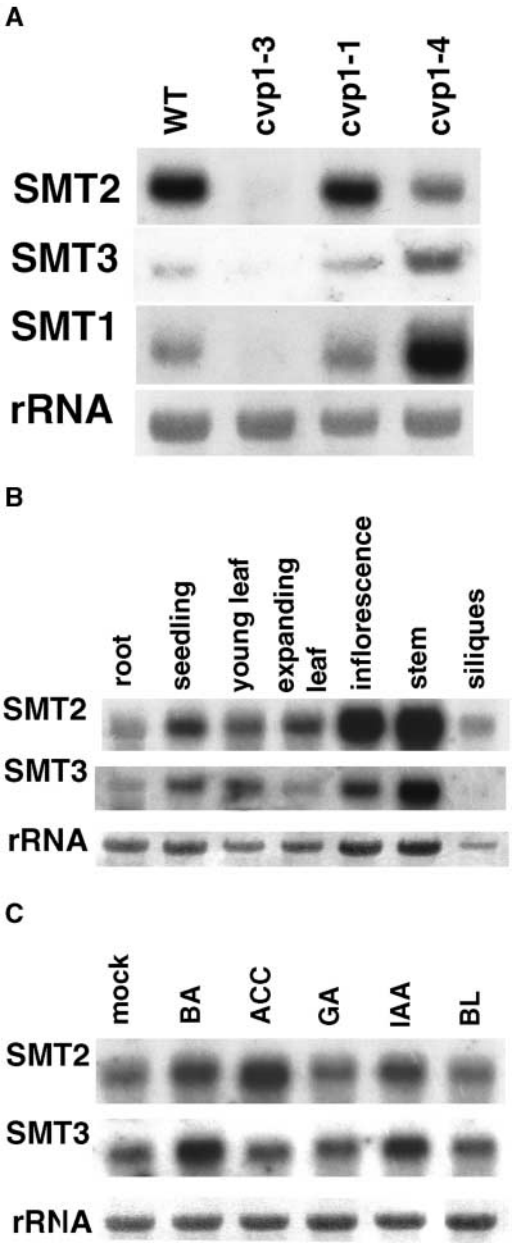

Figure 4. RNA Gel Blot Analysis of SMT.

(A) *SMT* transcript levels in different alleles (*SMT2*, *SMT3*, and *SMT1*) were hybridized sequentially to filters of the *cvp1* alleles subsequent to probe removal. RNA was isolated from 6-day-old seedlings. WT, wild type.

(B) *SMT2* and *SMT3* exhibit similar expression profiles. RNA was isolated from the indicated organ. Roots were excised from 1-week-old seedlings. Seedlings were 1 week old. Young leaves and expanding leaves were 2 to 3 mm and 4 to 5 mm in length, respectively. Siliques were from all developmental stages. Elongating regions of the stem were selected for RNA analysis.

(C) Tissue was incubated with the indicated hormone (see Methods). Mock, no hormone, BA, benzyladenine; ACC, 1-aminocyclopropane-1-carboxylic acid; GA, gibberellic acid; IAA, indoleacetic acid, BL, epibrassinolide. Ten micrograms of total RNA was loaded onto lanes. Methylene blue staining of rRNA served as the loading control. Only the top rRNA band is shown.

SMT2::*GUS* and *SMT3*::*GUS* flowers, staining was localized to the apical region of the sepal, particularly in the vascular bundles (Figures 6E and 6F). In *SMT2*::*GUS* siliques, GUS staining also was detected in ovules (Figure 6E). These data, in conjunction with the RNA gel blot analysis of organs and hormone application, indicate that *SMT2* and *SMT3* have similar but not identical expression patterns.

SMT2 and SMT3 Are Functionally Redundant

SMT2 and SMT3 are highly homologous, act on the same substrate, and exhibit similar but distinguishable expression patterns (Figures 4 and 6), suggesting that the proteins are functionally redundant. Because *SMT3* expression is restricted to the outer cell layers of the developing embryo, and thus is excluded from the majority of procambial cells of developing cotyledons (Diener et al., 2000), it appears that the function is provided solely by SMT2 in these locations. This probably explains the aberrant venation of *cvp1* mutants and provided an experimental system to test for functional redundancy in vivo.

We expressed either *SMT3* or *SMT2* in the *cvp1-1* background, under the control of the 35S promoter of *Cauliflower mosaic virus*, and observed full restoration of the vascular patterning, petal and sepal margin, and silique elongation defects in *cvp1-1* (Figures 7A to 7F and data not shown). However, the stem elongation defect was not rescued by *SMT3* (Figure 7G). This finding appears to reveal a role for SMT2 in the stem that is not shared by SMT3, indicating that the functional overlap is extensive but not complete.

SMT2 and *SMT3* have overlapping functions but are not completely functionally redundant. The overexpression of *SMT2* and *SMT3* yielded high transcript levels in the *cvp1-1* background but did not produce any phenotypic abnormalities (Figures 7H and 7I). In addition, *SMT2* overexpression did not have a detectable effect on *SMT3* transcript levels, and likewise, *SMT3* overexpression did not have an effect on *SMT2* transcript levels, indicating that the *cvp1* complementation is attributable specifically to *SMT3* ectopic expression. The overexpression of *SMT3* in the sense and antisense orientations in the wild-type background in ~60 transgenic plants also did not produce a phenotype (data not shown).

Based on the *SMT3* complementation of *cvp1* and the observation that *SMT3* is not expressed independently from *SMT2*, we propose that the lack of a phenotype in *SMT3* antisense plants is caused by the functional redundancy of

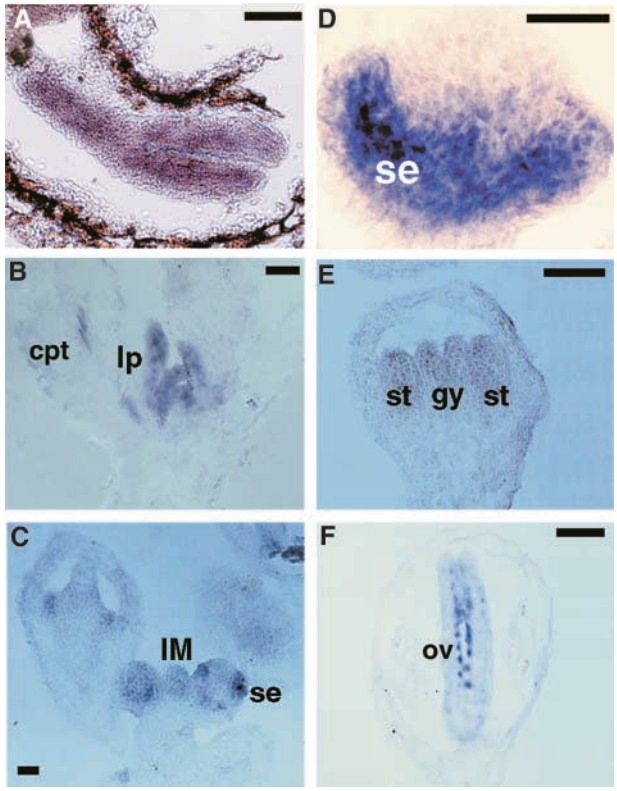

Figure 5. In Situ Localization of *SMT2* mRNA.

(A) *SMT2* is expressed throughout the developing embryo. Seed coat staining is background.
(B) Longitudinal section of a 7-day-old seedling to show *SMT2* expression in leaf primordia. The shoot apical meristem is not visible in this section.
(C) Longitudinal section of an inflorescence shows *SMT2* expression in the inflorescence meristem and sepals.
(D) Slightly oblique section of a stage 3 flower showing intense SMT2 expression in the sepals.
(E) Longitudinal section of a stage 5 to 6 flower reveals *SMT2* expression in stamens and in the gynoecium before fusion.
(F) Ovule expression of *SMT2*.
In **(C)** and **(E)** images were photographed with a blue filter. cpt, cotyledon petiole; gy, gynoecium; IM, inflorescence meristem; lp, leaf primordia; ov, ovules; se, sepals; st, stamens. Bars = 40 μm.

SMT2 and *SMT3*. This redundancy also may provide an explanation for the wild-type gross morphology of *cvp1-4*. *cvp1-4* has only 35% of SMT2 wild-type RNA levels and is predicted to have a truncated *SMT2* protein. However, increased levels of *SMT3* mRNA accumulate in this allele. We propose that the wild-type morphology of *cvp1-4* is maintained by the increase in SMT3 activity, which compensates for the decrease in SMT2 activity. The overlap in *SMT2* and *SMT3* expression patterns does not include the majority of cotyledon procambial cells, so a vascular patterning defect remains (Diener et al., 2000).

cvp1 Mutants Alter the Balance between Sterols and BRs

Because SMT2 catalyzes the methylation that distinguishes sterols from BRs, we determined whether the levels of sterol and BR intermediates were affected in the *cvp1* alleles. The levels of 22 sterol compounds were assayed in 1-week-old *cvp1-1*, *cvp1-3*, and *cvp1-4* seedlings (Table 1). Because whole seedlings were extracted for measurements, it is possible that individual cells and tissues exhibited significantly different values. In all tested alleles, the levels of intermediates before 24-methylenelophenol, the substrate of SMT2, were not altered significantly. By contrast, 24-methylenelophenol was increased in the *cvp1* mutants, and products of the sterol-specific pathway, such as 24-ethylidenelophenol, sitosterol, stigmasterol, and sitostanol, were decreased. 24-Methylenelophenol also was channeled into the BR pathway.

These precursors to the BRs were increased in *cvp1* relative to the wild type. For example, the null allele *cvp1-3* showed more than a 25-fold increase in 24-methylenecholesterol. Cholesterol lacks methyl additions and is formed by bypassing the methyl addition reactions. As predicted, cholesterol was higher in *cvp1* mutant alleles. Although there were gross changes in individual sterol levels, the total sterol content of *cvp1* was not markedly different from that of the wild type. Therefore, sterol levels were altered significantly in *cvp1*, most notably in the null allele *cvp1-3*, by shifting the balance of intermediates in favor of the BR pathway at the expense of the sterol pathway.

Because SMT2 regulates the biosynthetic flux that controls the amount of sterol and campesterol, the alteration in the flux often is expressed as a ratio of campesterol to sitosterol. In the wild type, this ratio was equal to 0.2, whereas in *cvp1*, the ratio was 1.9 or greater. In general, the decrease in sterol levels of the three alleles was proportional to the severity of their phenotypes. Although the *cvp1-3* null allele exhibited a reduction in transcript levels in all *SMT*s, it was able to produce alkylated sterols, albeit at reduced levels. The presence of sterols was reported in a null *smt1* allele (Diener et al., 2000). It is possible that lateral sterol pathways not normally used in wild-type sterol production are used in *smt1* and *cvp1* mutants.

The BR-Specific Inhibitor Brassinazole Does Not Rescue the *cvp1* Mutant Phenotype

All *cvp1* mutant alleles exhibited a decrease in sterols and a concomitant increase in the precursors to the BRs. Although BR levels were not assayed because of the large amount of

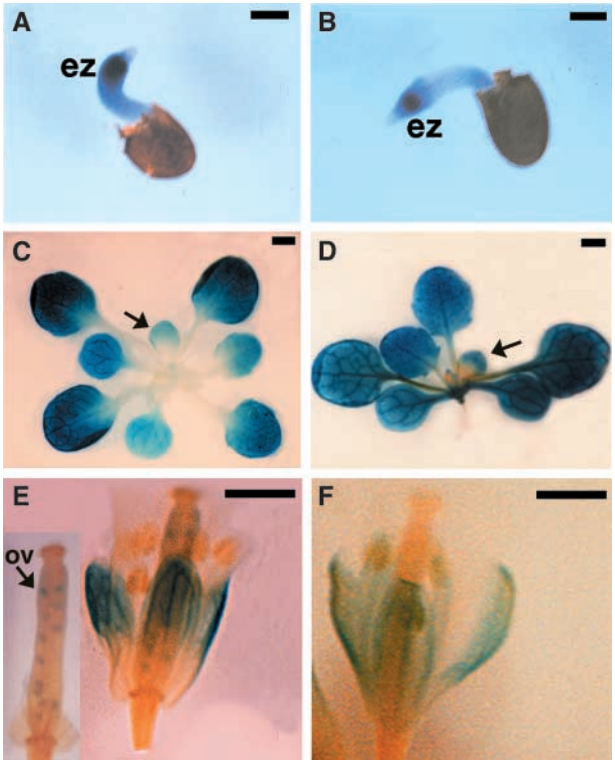

Figure 6. GUS Expression Studies of SMT2 and SMT3.

(A), **(C)**, and **(E)** *SMT2*::*GUS* reporter expression.
(B), **(D)**, and **(F)** *SMT3*::*GUS* reporter expression.
(A) and **(B)** Two-day-old germinated seedlings. Note the intense GUS staining in the elongation zone of the root.
(C) and **(D)** Plants with rosette leaves. In young leaves, GUS activity is restricted to the apical zone (arrows).
(E) and **(F)** Detached flowers show GUS enzyme activity in sepals, veins, and ovules (**[E]** only). For the inset in **(E)**, outer floral organs have been removed to expose the carpel.
ez, elongation zone; ov, ovules. Bars in **(A)** and **(B)** = 250 μm; bars in **(C)** to **(F)** = 2 mm.

tissue required, the *cvp1* sterol profile suggested that there was an increase in BR levels. Therefore, we determined whether the inhibition of the BR biosynthetic pathway could rescue any aspects of the *cvp1* phenotype. The *cvp1* vascular patterning defect occurs during embryogenesis. Thus, we applied the BR biosynthetic inhibitor brassinazole (Brz; Figure 3) (Asami and Yoshida, 1999) to soil-grown plants before bolting to test its effects on the stem internodal elongation defect.

As shown in Figure 8A, Brz application did not rescue this aspect of the mutant phenotype. Subsequent to treatment, seeds were isolated and the cotyledon vascular patterning defect was assessed in seedlings. Brz application during embryogenesis did not rescue the *cvp1* vascular patterning defect, nor did it affect the wild-type venation pattern (Figures 8B and 8C), suggesting that the phenotype is not the result of altered BR levels. The *cvp1* alleles exhibited a significant reduction in sitosterol and stigmasterol levels. We were unsuccessful in altering *cvp1* by supplementation with these compounds, although supplementation is made difficult by the limited solubility of the compounds.

DISCUSSION

The first recognizable event associated with the differentiation of provascular tissue is cell polarization and the formation of axialized procambial files. Our analysis of mutations that disrupt the *SMT2* gene demonstrates that this process is dependent on a functional sterol pathway. Arabidopsis has two very similar proteins (SMT2 and SMT3) acting at the same step in sterol biosynthesis, but only SMT2 is expressed in cotyledon vascular cells. This was important for two reasons. First, it allowed the critical observation of aberrant venation in the *cvp1* mutants, establishing a vascular role for the pathway. Second, it provided an experimental opportunity to introduce ectopic SMT3, demonstrating functional redundancy.

SMT2 acts at the bifurcation of the sterol and BR pathways, at which the substrate 24-methylenelophenol is methylated to enter the sterol pathway or is not further methylated and enters the BR pathway. Thus, SMT2 regulates the ratio of campesterol, precursor of the BRs, to sitosterol, the major sterol in plants. In *cvp1* mutants, we showed that this ratio, which normally favors the sterol pathway, was inverted to favor the BR pathway, possibly most dramatically in cotyledons. The phenotypic consequences could be the result of the enrichment of one or more BRs or of the depletion of one or more sterols, or a combination of both effects.

We favor the second of these possibilities. We believe that the potential increase of BR levels is unlikely to be the cause of the *cvp1* phenotype, for several reasons. First, we were unable to phenocopy the cotyledon vascular defect by supplementation of wild-type plants with brassinolide. Second, we were unable to cure the *cvp1* mutant phenotype by the application of Brz, an inhibitor that acts at a point in the BR pathway downstream from campesterol. Third, the BR pathway appears to be highly regulated, such that increases of early intermediates do not necessarily result in increased levels of the downstream active BR, brassinolide (Clouse and Sasse, 1998). Although we cannot exclude the possibility that BR alterations cause some of the *cvp1* phenotype, we believe it more likely that sterol depletions or modifications are responsible.

Sterols as membrane-ordering components are likely to have roles in organizing the many asymmetric structures and processes that are essential for the development of axialized files of polarized cells, such as the provascular cells and procambial strands that are affected in *cvp1* mutants. In addition, the sterol branch of the pathway may produce

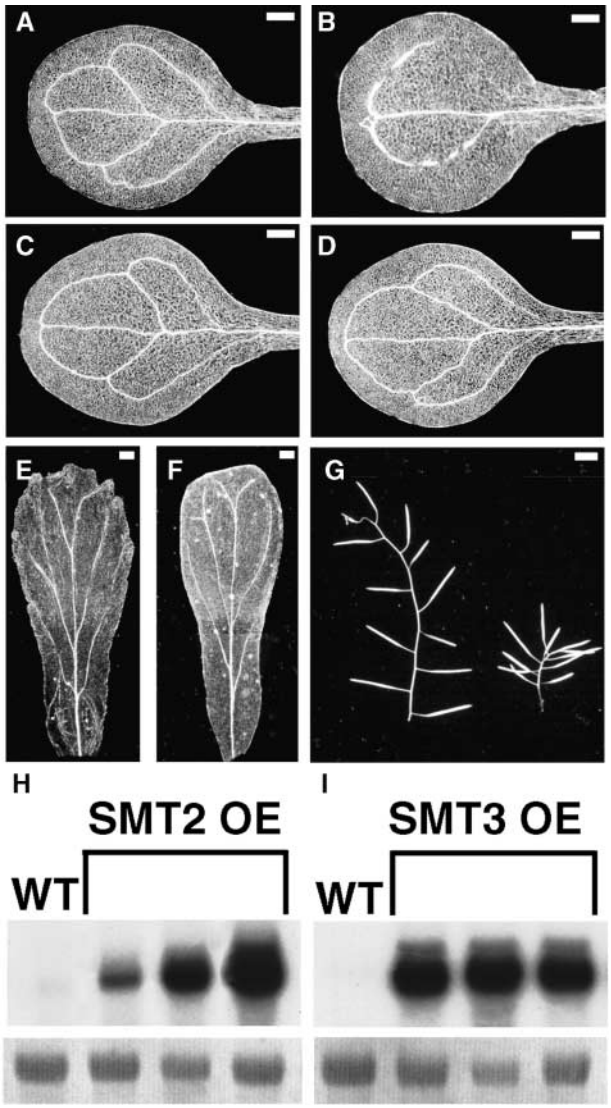

Figure 7. Functional Redundancy of SMT2 and SMT3.

(A) to **(F)** Cleared images of cotyledons (**[A]** to **[D]**) and petals (**[E]** and **[F]**) viewed under dark-field illumination. Bars = 250 μm.
(A) Wild type.
(B) *cvp1-1*.
(C) and **(D)** *cvp1-1* transformed with *35S/SMT2* **(C)** and *35S/SMT3* **(D)** to show complementation of the vascular patterning defect.
(E) and **(F)** *cvp1-1* petal with a scalloped apical region **(E)** and *cvp1-1* transformed with 35S/SMT3 **(F)** to show complementation of the petal defect.
(G) The stem internodal elongation defect is not rescued by SMT3 overexpression. A normal *cvp1-1* inflorescence stem is shown at left; an affected inflorescence stem of *cvp1-1*::*35S/SMT3* is shown at right. Three of 36 plants had affected inflorescences. Bar = 5 mm.
(H) and **(I)** RNA gel blot analysis of SMT2 **(H)** or SMT3 **(I)** overexpressors (OE). The first lane contains RNA from wild-type (WT) seedlings. The transcripts are weak as a result of a short exposure time. The next three lanes contain RNA isolated from three different SMT2 or SMT3 overexpressors. Each lane contained 5 μg of total RNA isolated from 9-day-old seedlings.

compounds distinct from BRs, with roles in intercellular signaling for the alignment of cell files and elongation axes or in conferring cell identity distinct from neighbor cells. We discuss each of these processes below in relation to the *cvp1* phenotype.

Role of SMT2 in Signaling

The *cvp1* venation defect may be the result of the absence or alteration of a sterol not identified previously as an intercellular or intracellular signal. Such a signal might serve to align provascular cells along an axis or to prevent neighboring cells from joining in the provascular cell fate. Vascular patterning is altered in several biosynthetic mutants that affect both sterols and BRs, including *fackel*, which is blocked upstream of the sterol/BR bifurcation, and *dwf7/ste1* (Choe et al., 1999b), which is blocked downstream. In addition, *bri1* mutants, with a defective BR receptor, also exhibit aberrant venation (Li and Chory, 1997; Wang et al., 2001). Unlike *cvp1*, these mutants generally show an overproliferation of phloem at the expense of xylem (Choe et al., 1999a). However, weak *fackel* alleles exhibit discontinuous venation patterns in cotyledons, similar to *cvp1* (Jang et al., 2000).

Although we did not measure brassinolide, the active signal in Arabidopsis, directly, it is unlikely that the *cvp1* defect is caused by excessive BR levels, for the reasons described above. Instead, another sterol-derived signal may be affected in *cvp1* and *fackel* mutants. There is indirect evidence for such signaling sterols in the spatial organization of various organs. Sterol/lipid binding domains (START) have been identified in a subtype of homeodomain/Leu zipper–containing proteins, which includes Athb-8, Athb-9, Athb-14, and REVOLUTA/INTERFASCICULAR FIBERLESS (Sessa et al., 1998; Zhong and Ye, 1999; Ratcliffe et al., 2000). In the case of the radial patterning genes *Phabulosa* (*phab*) and *Phavoluta* (*phav*), which encode the proteins ATHB-14 and ATHB-9, respectively, an unidentified sterol or lipid with spatial distribution is postulated to bind to the START domain of the receptors PHAB and PHAV to activate the genes involved in radial patterning (McConnell et al., 2001).

SMT2 and the Synthesis of Cellulose Microfibrils

The *cvp1* sitosterol deficiency might cause a vein pattern defect by interfering with the pattern of cellulose synthesis in the

Table 1. Sterol Profile of *cvp1* Alleles

	Genotype			
Sterol	Wild Type	*cvp1-1*	*cvp1-4*	*cvp1-3*
Cycloartenol	0.40	0.38	0.25	0.29
24-Methylenecycloartanol	0.49	0.45	0.25	0.29
Cycloeucalenol	0.26	0.34	0.22	0.29
Obtusifoliol	0.56	0.58	0.22	0.30
4α-Methyl-5α-ergosta-8, 14,24(28)-trien-3β-ol	0.03	0.03	0.02	0.03
24-Methylenelophenol	0.06	0.87	0.79	0.89
24-Ethylidenelophenol	0.35	0.13	0.10	0.12
Avenasterol	0.24	0.10	0.10	0.11
Isofucosterol	1.8	1.3	1.5	1.9
Sitosterol	91	39	32	26
Stigmasterol	8.8	3.9	5.0	4.5
Sitostanol	1.14	0.36	0.63	0.33
6-Oxositostanol	0.13	0.06	0.06	0.03
Episterol	0.053	0.42	0.38	0.63
24-Methylenecholesterol	0.27	2.90	2.62	6.82
Campesterol	19.2	72.3	67.5	68.9
Campestanol	0.33	1.01	1.31	1.30
6-Oxocampestanol	0.022	0.073	0.040	0.091
6-Deoxocathasterone	0.0031	0.0041	0.0031	0.0033
Cholesterol	1.9	4.2	3.4	6.7
Cholestanol	0.08	0.09	0.13	0.26
6-Oxocholestanol	0.02	0.03	0.02	0.03
Total sterol content	127.0	128.5	116.5	120.0
Ratio of campesterol to sitosterol[a]	0.21	1.9	2.2	2.6

Values are given in μg/g fresh weight.

[a] Values were converted to fraction of sterol/total sterol before calculating the ratio.

walls of provascular cells. Recently, the major plant sterol sitosterol was suggested as a primer for cellulose synthesis, which is initiated with the conjugation of Glc to sitosterol, forming sitosterol-β-glucoside (Peng et al., 2002). Further addition of Glc residues forms sitosterol cellodextrin, which is cleaved, allowing the transfer of the cellodextrin chain to another cellulase. After the attachment of additional Glc residues, the chain then assembles into cellulose microfibrils, which are the primary scaffolding component of plant cell walls and are postulated to orient the direction of cell expansion.

Because sitosterol is reduced greatly in *cvp1*, both sitosterol-β-glucoside and cellulose microfibrils might be reduced as a consequence, causing aberrations in the pattern of cell wall extensibility that normally guide the elongation and morphology of provascular and vascular cells. The aberrant cell expansion patterns observed in *cvp1* foliar organs and in *fackel* may be attributable to the same effects on cellulose priming. As discussed below, *cobra* mutants have reduced levels of cellulose and a concomitant alteration in cellulose microfibrils and cell expansion (Schindelman et al., 2001).

Lipid Rafts and the Compartmentalization of Proteins

In other systems, sterols have been shown to influence protein activity through their central role in organizing lipid rafts. Lipid rafts are membrane microenvironments that consist of dynamic compositions of sterols and lipids; they were identified initially in polarized epithelial and neuronal cells, in which they accumulate at a polar locality in the plasma membrane (Simons and Ikonen, 1997; Simons and Toomre, 2000). Through the inclusion or exclusion of specific proteins on the basis of affinity, rafts lead to the clustering of membrane-bound and membrane-associated proteins and serve as compartments for protein signaling complexes, cytoskeletal associations, channels, and other functional features of membranes. Numerous proteins, such as glucosylphosphatidylinositol (GPI)-linked proteins and transmembrane proteins, have been demonstrated to reside in such rafts. In many cases, sterol depletion results in the dissociation of membrane-bound proteins from lipid rafts, leading to mislocalization of the protein and/or inactivation of the signaling cascade (Simons and Toomre, 2000).

Rafts are assembled initially with endoplasmic reticulum–derived sterols in the Golgi, the site of lipid synthesis, and then are transported to the plasma membrane carrying proteins destined for polarized delivery. After protein delivery, rafts are endocytosed from the cell surface and then recycled either directly back to the plasma membrane or indirectly by endosomes. In plants, there are low sterol levels in the endoplasmic reticulum, where sterols are synthesized as corroborated by the presence of signal anchors on SMT2 and SMT3, and high levels in the plasma membrane, providing support for this mode of transport.

Although lipid rafts have not been observed in plants, their small size may have precluded observation by conventional microscopy. In other systems, raft components have been resolved through advanced microscopy techniques coupled with biochemical methods. Recently, a GPI-anchored protein was found to be the product of the Arabidopsis *COBRA* gene, whose mutant phenotype includes a loss of polarized, longitudinal expansion (Schindelman et al., 2001). The COBRA protein is localized asymmetrically in polarized cells, much like GPI-anchored proteins in other systems, and is postulated to play a role in oriented cell expansion, possibly through the recruitment of enzyme components involved in cellulose deposition. Although not demonstrated directly, this localization has the properties expected of a membrane raft-localized protein.

Other candidates for lipid raft localization in plants are the PIN family of auxin efflux carriers (Galweiler et al., 1998). Auxin flow is postulated to direct vascular cell patterning through the vectorial transport of auxin by basally localized efflux carriers. The mislocalization of a PIN efflux carrier in cotyledons of *cvp1* mutants might lead to the failure to form axialized files of provascular cells. PIN is cycled between the plasma membrane and an undefined endosomal compartment requiring ARF-GEF (Geldner et al., 2001) encoded

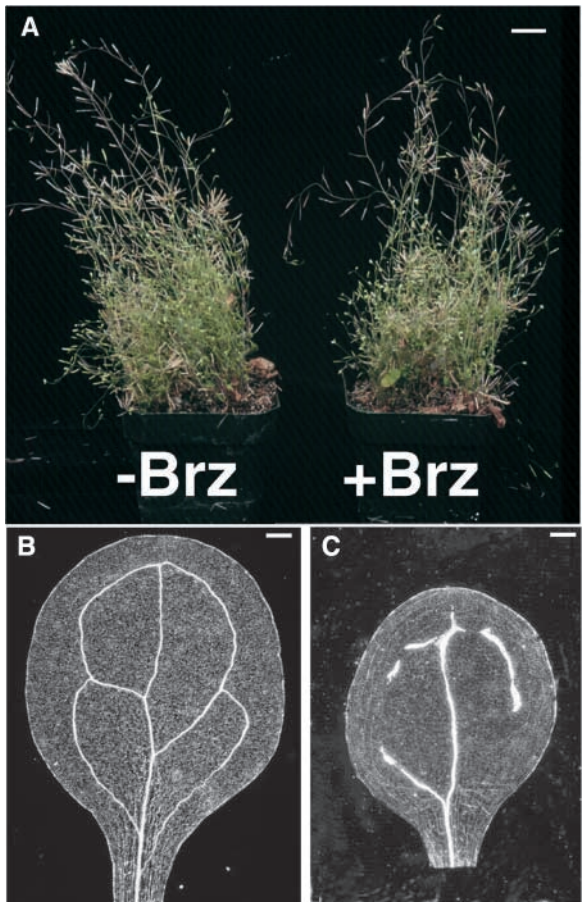

Figure 8. The BR Inhibitor Brz Does Not Rescue the *cvp1* Mutant Phenotype.

(A) Failure of Brz to rescue the stem elongation defect of *cvp1-3*. Note that there is no increase in plant height in Brz-treated *cvp1* plants relative to untreated *cvp1* plants.

(B) and **(C)**. Cleared cotyledons of wild-type **(B)** or *cvp1-3* **(C)** seedlings whose embryos were treated with Brz, viewed under dark-field illumination.

Plants were watered with 1 μM BRZ2001 (Sekimata et al., 2001) before bolting and until dessication. For **(B)** and **(C)** seed was collected from Brz-treated plants and germinated on Murashige and Skoog (1962) medium without Brz. Bar in **(A)** = 2.5 cm; bars in **(B)** and **(C)** = 100 μm.

by *EMB30/GNOM* (Shevell et al., 1994; Busch et al., 1996; Steinmann et al., 1999; Geldner et al., 2001). Although PIN-containing vesicles are not derived directly from the Golgi, such cycling is seen with other lipid raft-associated proteins.

It is tempting to speculate that PIN asymmetric delivery acts in association with lipid rafts. Alternatively, PIN may reside in plasma membrane microdomains rich in sterols and lipids. Although *pin* mutants have not been reported to exhibit any cotyledon vascular patterning discontinuities, *emb30/gnom* mutants exhibit a loss of vascular cell axialization similar to that observed in *cvp1* mutants, albeit much more severely (Mayer et al., 1993; Koizumi et al., 2000). There are many members of the PIN family, so functional redundancy probably exists. In *emb30/gnom*, vesicle transport–dependent polar localization of all PIN members would be affected; thus, a much more severe phenotype would occur.

Based on the known role of sterols in mammalian and yeast cells, it is likely that sterols act in more than one process. We propose that the *cvp1* mutant phenotype is not caused by a disruption in membrane permeability but rather reflects either (1) the mistargeting of proteins involved in polarizing and aligning vascular cells or (2) the synthesis of novel sterol signaling molecules. These two possibilities are not mutually exclusive. Sterol signaling may involve a receptor that subsequently initiates a signaling cascade that resides in a plasma membrane microdomain. The further analysis of *cvp1* and other sterol-defective mutants should reveal the roles of sterols in vascular pattern formation and other developmental processes.

METHODS

Plant Growth Conditions

All *cvp1* alleles were recovered from an ethyl methanesulfonate–mutagenized population of *Arabidopsis thaliana* ecotype Columbia in the screen described previously (Carland et al., 1999) and backcrossed at least three times. Seeds were surface-sterilized, plated on Murashige and Skoog (1962) (MS) medium (Sigma) with (for transgenic plants) or without antibiotics, and grown under continuous light. Approximately 1-week-old seedlings were either collected for RNA gel blot analysis, β-glucuronidase (GUS) staining, or sterol analysis or transplanted to soil and grown to maturity for additional manipulations. Wild-type and mutant plants were at the same developmental stage for comparative morphological studies. Plants in soil (Metromix; Scotts, Hope, AR) were grown at 22°C with a 16-h day and a light intensity of 200 $\mu mol \cdot m^{-2} \cdot s^{-1}$. The phenotype of *cvp1-3* plants grown at a higher light intensity (290 $\mu mol \cdot m^{-2} \cdot s^{-1}$) was not as severe.

Histology and GUS Histochemical Staining

To score cotyledon defects, one cotyledon was detached and cleared of chlorophyll by immersing cotyledon in fixative (ethanol:acetic acid [3:1]) and then rinsed in 70% and incubated in 100% ethanol at 4°C overnight. Cotyledons were viewed with a dissecting microscope. For photography, after the 100% ethanol dehydration step described above, specimens were further cleared by 1 h of incubation in 10% NaOH at 42°C and mounted in 50% glycerol. Vascular patterns were viewed under dark-field illumination using a Zeiss Axiophot microscope (Jena, Germany).

Plant organs were placed in 5-bromo-4-chloro-3-indolyl-β-glucuronic acid (X-Gluc) staining solution, infiltrated under vacuum for 10 min, wrapped in foil, and placed at 37°C. GUS staining was monitored for 2 to 12 h. X-Gluc staining solution of aerial organs contained

1 mM X-Gluc, 1 mM Na-phosphate buffer, pH 7.0, 1.0 mM EDTA, pH 8.0, 0.1% Triton X-100, 1 mM β-mercaptoethanol, 100 μg/mL chloramphenicol, 0.5 mM $K_3Fe(CN)_6$, and 0.5 mM $K_4Fe(CN)_6$. Improved specificity of X-Gluc staining in roots was obtained by following the method of Malamy and Benfey (1997). Samples were rinsed in 70% ethanol two times and mounted in 50% glycerol for photography using a Zeiss Stemi 2000-C dissecting microscope.

Positional Cloning of *CVP1*

cvp1-1 (ecotype Columbia) was crossed to Landsberg *erecta*. The resulting hybrid was self-pollinated to generate a large mapping population. Medium-grown F2 seedlings were scored for the mutant cotyledon vascular patterning phenotype. *cvp1* mutants were transferred subsequently to soil and allowed to mature. DNA was isolated from leaf tissue and scored for recombinants with the flanking cleaved amplified polymorphic markers g2395 and m59 (Hardtke and Berleth, 1998). Seeds were harvested from the *cvp1*/g2395 and *cvp1*/m59 recombinants. At this time, we noticed that *cvp1-1* in the Landsberg *erecta* background had a pleiotropic phenotype that included dwarfism and a severely stunted silique growth defect accompanied by a drastic reduction in fertility. This phenotype did not segregate with the Landsberg *erecta* mutation.

CVP1 was localized further by searching for polymorphic markers. To obtain new polymorphic markers, as BAC sequences became available in this region, 0.8-kb regions of DNA were amplified by PCR from Landsberg *erecta*, sequenced, and compared with the Columbia sequence. We designed several novel markers with this method and used them to further define the position of CVP1 to an ~150-kb region spanning two BACs. These markers are available upon request. Transformation-competent artificial chromosome (TAC) filters, obtained from the ABRC (Columbus, OH), were probed with 1-kb probes amplified from the unordered working-draft BAC sequences and hybridized using a formamide-based buffer, according to the protocol provided by Bio-Rad for Zetaprobe membranes. The positive TAC clones then were ordered into a TAC contig based on their hybridization signals.

Although eight TAC clones were transformed into *cvp1-1*, seeds were obtained from only five TAC clones because of low transformation frequency. Restriction analysis and gene annotation indicated the presence of six unique genes in a complementing TAC relative to an overlapping noncomplementing TAC. Upon sequencing *cvp1-1* alleles of these genes, a mutation was identified only in the *SMT2* gene. The remaining *cvp1* alleles were amplified by PCR, cloned into pCR2.1-TOPO vector (Invitrogen, Carlsbad, CA), and sequenced to identify base-pair changes within SMT2.

Plasmid Construction and Plant Transformation

All genes used in this study were PCR-amplified products from Arabidopsis ecotype Columbia that were introduced into pCR2.1-TOPO cloning vector, sequenced to ensure that there were no base-pair changes, and subcloned into the appropriate vector using compatible restriction sites within the polylinker. For complementation of *cvp1*, a genomic clone containing the 1.5-kb upstream region, coding region, and 3′ untranslated region using primers MT10 (5′-CGAGTGAGTCAGTCATAT-3′) and MT9 (5′-GTCAGTAGTGTTACTCACACAGGC-3′) was cloned into pCAMBIA 2300. For GUS constructs, 1.5-kb upstream regions of *SMT2* (MT10 and MT7 [5′-CGTTAAGAGTGAGGAAGACC-3′]) or SMT3 (SMT3-1 [5′-CACAGGGAGAAAGAGAGAAGC-3′] and SMT3-2 [5′-CGTGTGAGCAAATAGATCACG-3′]) were cloned into both pBI101 (Clontech, Palo Alto, CA) and pCAMBIA 1381.

For overexpression of SMT2 or SMT3, because there are no introns, a genomic region representing the cDNA of *SMT2* (MT1 [5′-GGTCTTCCTCACTCTTAACG-3′] and MT9) or *SMT3* (SMT3-6 [5′-CAGAGTCGTGAACTTAACG-3′] and SMT3-7 [5′-CCAATAGAATTTCCCGGC-3′]) was amplified by PCR and eventually cloned into pZP35 (Hajdukiewicz et al., 1994) that had been engineered with a nopaline synthase 3′ terminator sequence. *SMT3* cDNA also was introduced in the antisense orientation in pZP35nos. Additional information on the design of these constructs will be provided upon request. For each construct, 25 to 60 transgenic plants were analyzed for GUS histochemistry or phenotype and/or RNA gel blot analysis.

Plant transformations were conducted (Bechtold and Pelletier, 1998) with modifications (Clough and Bent, 1998).

Hormone Induction Studies and RNA Gel Blot Analysis

For hormone induction experiments, a modification of a method described previously (Gil et al., 1994) was used. One-week-old light-grown seedlings were cut into 0.5-cm pieces and incubated in 0.5 × MS salts, 1% Suc, and 50 μM cycloheximide. After 4 h of incubation at room temperature, the buffer was replaced with fresh buffer containing the appropriate hormone and incubated for an additional 2 h. The tissue then was blotted dry with tissue paper, frozen in liquid N_2, and stored at −70°C. Hormone levels were as follows: 20 μM indoleacetic acid, 20 μM benzyladenine, 50 μM gibberellic acid, 20 μM 1-aminocyclopropane-1-carboxylic acid, and 2 μM 24-epibrassinolide. Indoleacetic acid, gibberellic acid, 1-aminocyclopropane-1-carboxylic acid, and benzyladenine were obtained from Sigma. 24-Epibrassinolide was obtained from CIDtech Research (Cambridge, Ontario, Canada). The experiment was conducted two times and yielded the same results.

For RNA gel blot analysis, RNA was isolated using the Trizol method (Gibco BRL). Unless noted otherwise, 10 μg of RNA was loaded onto formaldehyde gels, electrophoresed under denaturing conditions, and transferred to a nylon membrane (Zetaprobe; Bio-Rad). To ensure equal loading of RNA, filters were stained in 0.02% methylene blue and 0.3 M NaOAc, pH 5.5, according to a published method (Herrin, 1988). After cross-linking RNA to filter, the filters were hybridized to gene-specific probes (SMT2, MT1 and MT9; SMT3, SMT3-6 and SMT3-7; SMT1, SMT1-1 [5′-CTCCGATTCATCTTTATCCTC-3′] and SMT1-2 [5′-GGGCATGTGCACATGATTCAG-3′]) using a formamide-based hybridization buffer according to the manufacturer's protocol (Bio-Rad). After hybridization, filters were washed in 0.5 × wash buffer (0.075 M NaCl, 0.0075 M Na-citrate, 2.5% SDS, and 0.05% NaPPi) at 55°C. Under these conditions, there was no cross-hybridization between probes. SMT1 was amplified from 1-week-old seedling RNA using the 5′ rapid amplification of cDNA ends system (Gibco BRL) for first-strand synthesis. Density measurements were made using Image Gauge version 3.3 (Fuji Photo Film Co., Tokyo, Japan).

RNA in Situ Hybridization

A full-length *SMT2* probe and the *SMT2* 3′ untranslated region (MT11 [5′-GGTAGAAAGGAAACATCACCGG-3′] and MT9) were cloned into

pBluescript II SK+ (Stratagene) in both orientations and digested with the appropriate enzyme (BamHI) to yield templates for sense and antisense in vitro transcription according to the manufacturer's suggestions (Roche, Indianapolis, IN). In situ hybridization experiments were conducted (Long et al., 1996) with a hybridization temperature of 42°C. The *SMT2* 3′ untranslated region probe yielded the same signal as the full-length probe and did not hybridize with *SMT3*. The signal was apparent after 2 days. Sense controls showed no signal. Photography was conducted using a Zeiss Axiophot microscope.

Measurement of Sterol Levels

Levels of 22 sterol intermediates were assayed from 1-week-old seedlings. Plant tissue was frozen and lyophilized before extraction, purification, and gas chromatography–mass spectrometry analysis (Noguchi et al., 1999).

Upon request, all novel materials described in this article will be made available in a timely manner for noncommercial research purposes. No restrictions or conditions will be placed on the use of any materials described in this article that would limit their use for noncommercial research purposes.

Accession Number

Accession numbers for pCAMBIA 2300 and 1381 plasmids are AF234315 and AF234302, respectively.

ACKNOWLEDGMENTS

We are grateful to Brian Keith (University of Pennsylvania) for providing the *cvp1* alleles and to Asami Tadao (Institute of Physical and Chemical Research) for providing Brz. We thank Lien Lai (Ohio State University) for advice on positional cloning. We gratefully acknowledge Neil McHale (Connecticut Agricultural Experiment Station) for a critical review of the manuscript. We acknowledge the ABRC for providing the TAC filter and BAC and TAC clones used in the cloning of *CVP1*. This research was supported by Grants IBN-9808295 and IBN-0110730 from the National Science Foundation.

Received April 18, 2002; accepted May 27, 2002.

REFERENCES

Asami, T., and Yoshida, S. (1999). Brassinosteroid biosynthesis inhibitors. Trends Plant Sci. **4,** 348–353.

Bechtold, N., and Pelletier, G. (1998). In planta Agrobacterium-mediated transformation of adult *Arabidopsis thaliana* plants by vacuum infiltration. Methods Mol. Biol. **82,** 259–266.

Benveniste, P. (1986). Sterol biosynthesis. Annu. Rev. Plant Physiol. **37,** 275–308.

Bouvier-Nave, P., Husselstein, T., Desprez, T., and Benveniste, P. (1997). Identification of cDNAs encoding sterol methyl-transferases involved in the second methylation step of plant sterol biosynthesis. Eur. J. Biochem. **246,** 518–529.

Busch, M., Mayer, U., and Jurgens, G. (1996). Molecular analysis of the Arabidopsis pattern formation of gene GNOM: Gene structure and intragenic complementation. Mol. Gen. Genet. **250,** 681–691.

Carland, F.M., Berg, B.L., FitzGerald, J.N., Jinamornphongs, S., Nelson, T., and Keith, B. (1999). Genetic regulation of vascular tissue patterning in Arabidopsis. Plant Cell **11,** 2123–2137.

Carland, F.M., and McHale, N.A. (1996). LOP1: A gene involved in auxin transport and vascular patterning in Arabidopsis. Development **122,** 1811–1819.

Choe, S., Dilkes, B.P., Gregory, B.D., Ross, A.S., Yuan, H., Noguchi, T., Fujioka, S., Takatsuto, S., Tanaka, A., Yoshida, S., Tax, F.E., and Feldmann, K.A. (1999a). The Arabidopsis dwarf1 mutant is defective in the conversion of 24-methylenecholesterol to campesterol in brassinosteroid biosynthesis. Plant Physiol. **119,** 897–907.

Choe, S., Noguchi, T., Fujioka, S., Takatsuto, S., Tissier, C.P., Gregory, B.D., Ross, A.S., Tanaka, A., Yoshida, S., Tax, F.E., and Feldmann, K.A. (1999b). The Arabidopsis dwf7/ste1 mutant is defective in the delta7 sterol C-5 desaturation step leading to brassinosteroid biosynthesis. Plant Cell **11,** 207–221.

Choe, S., Tanaka, A., Noguchi, T., Fujioka, S., Takatsuto, S., Ross, A.S., Tax, F.E., Yoshida, S., and Feldmann, K.A. (2000). Lesions in the sterol delta reductase gene of Arabidopsis cause dwarfism due to a block in brassinosteroid biosynthesis. Plant J. **21,** 431–443.

Clough, S.J., and Bent, A.F. (1998). Floral dip: A simplified method for Agrobacterium-mediated transformation of *Arabidopsis thaliana*. Plant J. **16,** 735–743.

Clouse, S.D., and Sasse, J.M. (1998). Brassinosteroids: Essential regulators of plant growth and development. Annu. Rev. Plant Physiol. Plant Mol. Biol. **49,** 427–451.

Cnops, G., Wang, X., Linstead, P., Van Montagu, M., Van Lijsebettens, M., and Dolan, L. (2000). Tornado1 and tornado2 are required for the specification of radial and circumferential pattern in the Arabidopsis root. Development **127,** 3385–3394.

Deyholos, M.K., Cordner, G., Beebe, D., and Sieburth, L.E. (2000). The SCARFACE gene is required for cotyledon and leaf vein patterning. Development **127,** 3205–3213.

Diener, A.C., Li, H., Zhou, W., Whoriskey, W.J., Nes, W.D., and Fink, G.R. (2000). Sterol methyltransferase 1 controls the level of cholesterol in plants. Plant Cell **12,** 853–870.

Galweiler, L., Guan, C., Muller, A., Wisman, E., Mendgen, K., Yephremov, A., and Palme, K. (1998). Regulation of polar auxin transport by AtPIN1 in Arabidopsis vascular tissue. Science **282,** 2226–2230.

Geldner, N., Friml, J., Stierhof, Y.D., Jurgens, G., and Palme, K. (2001). Auxin transport inhibitors block PIN1 cycling and vesicle trafficking. Nature **413,** 425–428.

Gil, P., Liu, Y., Orbovic, V., Verkamp, E., Poff, K.L., and Green, P.J. (1994). Characterization of the auxin-inducible SAUR-AC1 gene for use as a molecular genetic tool in Arabidopsis. Plant Physiol. **104,** 777–784.

Grebe, M., Gadea, J., Steinmann, T., Kientz, M., Rahfeld, J.U., Salchert, K., Koncz, C., and Jurgens, G. (2000). A conserved domain of the Arabidopsis GNOM protein mediates subunit interaction and cyclophilin 5 binding. Plant Cell **12,** 343–356.

Hajdukiewicz, P., Svab, Z., and Maliga, P. (1994). The small, versatile pZP family of Agrobacterium binary vectors for plant transformation. Plant Mol. Biol. **25,** 989–994.

Hardtke, C.S., and Berleth, T. (1998). The Arabidopsis gene

MONOPTEROS encodes a transcription factor mediating embryo axis formation and vascular development. EMBO J. **17,** 1405–1411.

Hartmann, M.-A. (1998). Plant sterols and the membrane environment. Trends Plant Sci. **3,** 170–175.

Herrin, D.L. (1988). Rapid, reversible staining of northern blots prior to hybridization. Biotechniques **6,** 196–198.

Husselstein, T., Gachotte, D., Desprez, T., Bard, M., and Benveniste, P. (1996). Transformation of *Saccharomyces cerevisiae* with a cDNA encoding a sterol C-methyltransferase from *Arabidopsis thaliana* results in the synthesis of 24-ethyl sterols. FEBS Lett. **381,** 87–92.

Jang, J.C., Fujioka, S., Tasaka, M., Seto, H., Takatsuto, S., Ishii, A., Aida, M., Yoshida, S., and Sheen, J. (2000). A critical role of sterols in embryonic patterning and meristem programming revealed by the fackel mutants of *Arabidopsis thaliana*. Genes Dev. **14,** 1485–1497.

Klahre, U., Noguchi, T., Fujioka, S., Takatsuto, S., Yokota, T., Nomura, T., Yoshida, S., and Chua, N.H. (1998). The Arabidopsis DIMINUTO/DWARF1 gene encodes a protein involved in steroid synthesis. Plant Cell **10,** 1677–1690.

Koizumi, K., Sugiyama, M., and Fukuda, H. (2000). A series of novel mutants of *Arabidopsis thaliana* that are defective in the formation of continuous vascular network: Calling the auxin signal flow canalization hypothesis into question. Development **127,** 3197–3204.

Li, J., and Chory, J. (1997). A putative leucine-rich repeat receptor kinase involved in brassinosteroid signal transduction. Cell **90,** 929–938.

Liu, Y.G., Shirano, Y., Fukaki, H., Yanai, Y., Tasaka, M., Tabata, S., and Shibata, D. (1999). Complementation of plant mutants with large genomic DNA fragments by a transformation-competent artificial chromosome vector accelerates positional cloning. Proc. Natl. Acad. Sci. USA **96,** 6535–6540.

Long, J.A., Moan, E.I., Medford, J.I., and Barton, M.K. (1996). A member of the KNOTTED class of homeodomain proteins encoded by the STM gene of Arabidopsis. Nature **379,** 66–69.

Malamy, J.E., and Benfey, P.N. (1997). Organization and cell differentiation in lateral roots of *Arabidopsis thaliana*. Development **124,** 33–44.

Mayer, U., Büttner, G., and Jurgens, G. (1993). Apical-basal pattern formation in the Arabidopsis embryo: Studies on the role of the *gnom* gene. Development **117,** 149–162.

McConnell, J.R., Emery, J., Eshed, Y., Bao, N., Bowman, J., and Barton, M.K. (2001). Role of PHABULOSA and PHAVOLUTA in determining radial patterning in shoots. Nature **411,** 709–713.

Murashige, T., and Skoog, F. (1962). A revised medium for rapid growth and bioassays with tobacco tissue culture. Physiol. Plant. **15**, 473–497.

Nelson, T., and Dengler, N. (1997). Leaf vascular pattern formation. Plant Cell **9,** 1121–1135.

Nes, W.D., McCourt, B.S., Marshall, J.A., Ma, J., Dennis, A.L., Lopez, M., Li, H., and He, L. (1999). Site-directed mutagenesis of the sterol methyltransferase active site from *Saccharomyces cerevisiae* results in formation of novel 24-ethyl sterols. J. Org. Chem. **64,** 1535–1542.

Noguchi, T., Fujioka, S., Takatsuto, S., Sakurai, A., Yoshida, S., Li, J., and Chory, J. (1999). Arabidopsis det2 is defective in the conversion of (24R)-24-methylcholest-4-en-3-one to (24R)-24-methyl-5alpha-cholestan-3-one in brassinosteroid biosynthesis. Plant Physiol. **120,** 833–840.

Parks, L.W., Crowley, J.H., Leak, F.W., Smith, S.J., and Tomeo, M.E. (1999). Use of sterol mutants as probes for sterol functions in the yeast, *Saccharomyces cerevisiae*. Crit. Rev. Biochem. Mol. Biol. **34,** 399–404.

Peng, L., Kawagoe, Y., Hogan, P., and Delmer, D. (2002). Sitosterol-beta-glucoside as primer for cellulose synthesis in plants. Science **295,** 147–150.

Przemeck, G.K., Mattsson, J., Hardtke, C.S., Sung, Z.R., and Berleth, T. (1996). Studies on the role of the Arabidopsis gene MONOPTEROS in vascular development and plant cell axialization. Planta **200,** 229–237.

Ratcliffe, O.J., Riechmann, J.L., and Zhang, J.Z. (2000). INTERFASCICULAR FIBERLESS1 is the same gene as REVOLUTA. Plant Cell **12,** 315–317.

Schaeffer, A., Bronner, R., Benveniste, P., and Schaller, H. (2001). The ratio of campesterol to sitosterol that modulates growth in Arabidopsis is controlled by STEROL METHYLTRANSFERASE 2;1. Plant J. **25,** 605–615.

Schindelman, G., Morikami, A., Jung, J., Baskin, T.I., Carpita, N.C., Derbyshire, P., McCann, M.C., and Benfey, P.N. (2001). COBRA encodes a putative GPI-anchored protein, which is polarly localized and necessary for oriented cell expansion in Arabidopsis. Genes Dev. **15,** 1115–1127.

Schrick, K., Mayer, U., Horrichs, A., Kuhnt, C., Bellini, C., Dangl, J., Schmidt, J., and Jurgens, G. (2000). FACKEL is a sterol C-14 reductase required for organized cell division and expansion in Arabidopsis embryogenesis. Genes Dev. **14,** 1471–1484.

Sekimata, K., Kimura, T., Kaneko, I., Nakano, T., Yoneyama, K., Takeuchi, Y., Yoshida, S., and Asami, T. (2001). A specific brassinosteroid biosynthesis inhibitor, Brz2001: Evaluation of its effects on Arabidopsis, cress, tobacco, and rice. Planta **213,** 716–721.

Sessa, G., Steindler, C., Morelli, G., and Ruberti, I. (1998). The Arabidopsis Athb-8, -9 and -14 genes are members of a small gene family coding for highly related HD-ZIP proteins. Plant Mol. Biol. **38,** 609–622.

Shevell, D.E., Leu, W.M., Gillmor, C.S., Xia, G., Feldmann, K.A., and Chua, N.H. (1994). EMB30 is essential for normal cell division, cell expansion, and cell adhesion in Arabidopsis and encodes a protein that has similarity to Sec7. Cell **77,** 1051–1062.

Simons, K., and Ikonen, E. (1997). Functional rafts in cell membranes. Nature **387,** 569–572.

Simons, K., and Toomre, D. (2000). Lipid rafts and signal transduction. Nat. Rev. Mol. Cell Biol. **1,** 31–39.

Sitbon, F., and Jonsson, L. (2001). Sterol composition and growth of transgenic tobacco plants expressing type-1 and type-2 sterol methyltransferases. Planta **212,** 568–572.

Steinmann, T., Geldner, N., Grebe, M., Mangold, S., Jackson, C.L., Paris, S., Galweiler, L., Palme, K., and Jurgens, G. (1999). Coordinated polar localization of auxin efflux carrier PIN1 by GNOM ARF GEF. Science **286,** 316–318.

Wang, Z.Y., Seto, H., Fujioka, S., Yoshida, S., and Chory, J. (2001). BRI1 is a critical component of a plasma-membrane receptor for plant steroids. Nature **410,** 380–383.

Zhong, R., and Ye, Z.H. (1999). IFL1, a gene regulating interfascicular fiber differentiation in Arabidopsis, encodes a homeodomain-leucine zipper protein. Plant Cell **11,** 2139–2152.